WAVE PROPAGATION AND RESPONSE STATISTICS OF SHORT FIBRE COMPOSITES FROM EXPERIMENTAL ESTIMATION OF MATERIAL PROPERTIES

CONFERENCE PAPER · DECEMBER 2015

Adriano Fabro

University of Brasília

N. S. Ferguson

Institute of Sound and Vibration Research

Brian Mace

University of Auckland

23rd ABCM International Congress of Mechanical Engineering
December 6-11, 2015, Rio de Janeiro, RJ, Brazil

WAVE PROPAGATION AND RESPONSE STATISTICS OF SHORT FIBRE COMPOSITES FROM EXPERIMENTAL ESTIMATION OF MATERIAL PROPERTIES

Adriano T. Fabro
Department of Mechanical Engineering, University of Brasilia, Brasília-DF, 70910-900, Brazil
fabro@unb.br

Neil S. Ferguson
ISVR, University of Southampton, Highfield Campus, Southampton, SO17 1BJ, United Kingdom
nsf@isvr.soton.ac.uk

Brian. R. Mace
Department of Mechanical Engineering, University of Auckland, Private Bag 92019, Auckland 1142, New Zealand
b.mace@auckland.ac.nz

Abstract. *Typically there is variability in the material and geometrical properties of fibre-reinforced composites and this variability is often spatially correlated. Numerical models can predict the response of such panels, but the spatially correlated nature of the variability must be represented within the model. However, characterising the variability, and especially the spatial correlation, is problematic. In this study data is first generated by an automated optical process: light transmissibility measurements are taken of a dry chopped strand mat panel. The intensity of the consequent image is post-processed to describe the fibre density as a random field using the Karhunen-Loeve decomposition. The panel is then cut into beams, from which mobility measurements are taken, providing an ensemble of mobility and natural frequency information. The WKB (after Wentzel, Kramers and Brillouin) approximation, is used in order to find a suitable wave solutions for finite waveguides considering the given random field. Subsequent realisations of the random field are then used to predict the statistics of the vibration response of the beams. Numerical and experimental results show a very good agreement. This approach significantly reduces the computational time when compared to standard Finite Element calculations and provides a suitable framework to account for randomness in the properties.*

Keywords: *Fibre Reinforcement; Random Fields; Karhunen-Loeve Expansion; WKB approximation; Experimental Validation*

1. INTRODUCTION

Manufacturing processes often result in a variability of the properties compared to the nominal designed product. As the requirements for optimum design increase, it might be important to improve the prediction capability by incorporating such features. It is usual that the mechanical properties of composite structures are modelled by analytical models taking into account the mean properties in the structure, although they can exhibit great spatial variability.

The characterisation of the spatial variability becomes even more relevant when dealing with fibre reinforced composite materials, for instance, for which different fibre arrangements can affect the mechanical properties (Lei et al., 2012) and high material correlation is expected from the variability in physical features such as the fibre volume fraction (Smarslok et al., 2012). Moreover, the use of a purely deterministic approach to model and, consequently, design structures using these materials can limit their applicability and require higher safety factors (Sriramula and Chryssanthopoulos, 2009). Even though the inclusion of spatial variability and uncertainties in mechanical models has received significant attention, for instance (Der Kiureghian and Ke, 1988, Gangadhar and Zehn, 2007, Ghanem and Spanos, 2012, Schueller, 1997, Stefanou, 2009, Sudret and Der Kiureghian, 2000, Zehn and Saitov, 2003), it is very difficult to quantify the spatial variation of material properties by procedures involving, for instance, manual measurement. A few experimental procedures for characterisation of the spatial variability in fibre reinforced composite materials have been recently proposed, based on the volume fraction or fibre distribution.

The higher the frequency range under analysis using Finite Elements (FE), the finer the mesh requirement, with increased computational cost. The pollution effect, i.e. when the accuracy of the FE solution degenerates as the wavenumber or frequency increases (Deraemaeker et al., 1999), must also be taken into account, further increasing the computational cost. Besides, even small variability starts to play an important role such that a deterministic FE approach by itself is no longer able to predict the structure's behaviour accurately. It is then necessary to add some level of randomness within the description of the structural models and therefore increasing the computational cost further.

Wave-based methods have been developed in order to attempt to overcome this limitation of the FE approach, bridging the called mid-frequency gap in the prediction tools, by increasing computational efficiency, and therefore extend the applicability of the deterministic models to higher frequencies. However, most of them assume that waveguide properties are homogeneous in the direction of the travelling wave, limiting the application of such approaches. Such limitations arise mainly because analytical solutions for non-homogeneous waveguides are only possible for very particular cases, for example acoustic horns, ducts, rods and beams - e.g. (Eisenberger, 1991, Guo and Yang, 2012, Li, 2000) - particularly when the variation in the properties of the waveguide over distances to the wavelength are small.

In section 2 the WKB approximation for the wave solution is briefly reviewed and used along with a generalized approach for one-dimensional waveguides in terms of propagation, reflection and transmission matrices, as found in (Fabro et al., 2015b). This approximation requires that the internal reflections are negligible or none due to any local changes in the material or geometrical properties. In section 3, an experimental procedure for estimating random field properties of a glass-fibre reinforced epoxy composite material is briefly reviewed and the main results are presented for two different panels. Section 4 presents the experimental procedure for estimating natural frequencies of an ensemble of beams cut from each panel and section 5 presents the results and discussion comparing the statistics of the natural frequencies obtained from the WKB approach using the estimated random field and from the experimental procedure. Finally, section 6 draws some final remarks.

2. THE WKB APPROXIMATION

The classical WKB approximation, a method for finding suitable modifications of plane-wave solutions for propagation in slowly varying media (Pierce, 1970), named after Wentzel, Kramers and Brillouin, was initially developed for solving the Schrödinger equation in quantum mechanics. The formulation assumes that the waveguide properties vary slowly enough such that there are no or negligible reflections due to these locals changes, even if the net change is big. It has been applied in many fields of engineering, including ocean acoustics (Jensen et al., 2011), acoustics (Arenas and Crocker, 2001, Gaulter and Biggs, 2012, Rienstra, 2003) and structural dynamics (Firouz-Abadi et al., 2007, Pierce, 1970). However, the WKB approximation breaks down when the travelling wave reaches a local cut-off section where the wave mode ceases to propagate. This transition, also known as a turning point, leads to an internal reflection, breaking down the main assumption in the theory, requiring a different approximation for certain frequency bands (e.g. (Nayfeh, 1973)).

Assuming a time harmonic solution, $u(x,t) = U(x)\, e^{-i\omega t}$ for the displacement response, it is possible to define a local wavenumber $k(x)$. Thus, the *eikonal* function $S(x) = \ln \widetilde{U}(x) + i\theta(x)$ is introduced, in order to find wave solutions of the kind $U(x) = e^{S(x)} = \widetilde{U}(x)e^{\pm i\theta(x)}$. A formulation in terms of propagation matrices $\mathbf{\Lambda}$ and reflection matrices $\mathbf{\Gamma}$ for the WKB approach is reviewed and used for the particular results of a beam (Fabro et al., 2015b). The wave vector amplitudes are given by $\mathbf{a}_j = \left[\mathbf{a}_j^+ \quad \mathbf{a}_j^-\right]^T$ and $\mathbf{b}_j = \left[\mathbf{b}_j^+ \quad \mathbf{b}_j^-\right]^T$, where the propagating and evanescent waves are, respectively, given as $\mathbf{a}_j^+ = \left[\mathrm{a}_j^+ \quad \mathrm{a}_{Nj}^+\right]^{\mathrm{T}}$, $\mathbf{a}_j^- = [\mathrm{a}_j^- \quad \mathrm{a}_{Nj}^-]^{\mathrm{T}}$, $\mathbf{b}_j^+ = \left[\mathrm{b}_j^+ \quad \mathrm{b}_{Nj}^+\right]^{\mathrm{T}}$ and $\mathbf{b}_j^- = [\mathrm{b}_j^- \quad \mathrm{b}_{Nj}^-]^{\mathrm{T}}$, for $j = 1,2$. The matrices $\mathbf{\Lambda_{11}}$ and $\mathbf{\Lambda_{22}}$ are the diagonal elements of the propagation matrix $\mathbf{\Lambda}$.

The waveguide natural frequencies can be determined by applying the wave train closure principle, tracing the round-trip propagating wave (Cremer et al., 2010). Considering a one dimensional finite waveguide with length L, then the positive going $\mathbf{a}^+$ and the negative going $\mathbf{a}^-$ wave amplitude vectors on the left and on hand boundary, $\mathbf{b}^+$ and $\mathbf{b}^-$, can be related by the propagation matrix $\mathbf{b} = \mathbf{\Lambda a}$. The waves reflected from boundaries at the left and the right hand ends are given by the respective reflection matrices as $\mathbf{a}^+ = \mathbf{\Gamma_L a}^-$ and $\mathbf{b}^- = \mathbf{\Gamma_R b}^+$. Thus, $\mathbf{b}^+ = \mathbf{\Lambda_{11} a}^+$ and $\mathbf{b}^- = \mathbf{\Lambda}_{22}\mathbf{a}^-$, and using the reflection relations at the boundaries, then $\mathbf{b}^+ = \mathbf{\Lambda_{11}\Gamma_L a}^-$ and $\mathbf{\Gamma_R b}^+ = \mathbf{\Lambda_{22} a}^-$**,** where $(\cdot)_{\boldsymbol{ij}}$ is the i^{th} row and j^{th} column block element of the partitioned matrix. Applying the wave train closure principle, for energy conserving boundaries and tracing the round-trip propagating wave, the natural frequencies correspond to the zeros of the characteristic equation (Cremer et al., 2010, Mace, 1984)

$$\det|\mathbf{\Lambda}_{22}^{-1}\mathbf{\Gamma}_R\mathbf{\Lambda}_{11}\mathbf{\Gamma}_L - \mathbf{I}| = 0, \tag{1}$$

where $\mathbf{I}$ is the identity matrix, and $(\cdot)_{\boldsymbol{ij}}$ is the i^{th} row and j^{th} column block matrix of the corresponding propagation matrix. The forced response can also be calculated following the same rationale (Fabro et al., 2015b).

This procedure can be applied to an Euler-Bernoulli beam where $EI_{yy} = E(x)I_{yy}(x)$ and $\rho A = \rho(x)A(x)$ are the spatially varying flexural stiffness and mass per unit length, respectively, and $w(x,t)$ is the transverse displacement along the beam. Assuming a time harmonic solution $w(x,t) = W(x)e^{-i\omega t}$, then the WKB approach is used to find wave solutions of the kind $W(x) = \widetilde{W}(x)e^{\pm i\theta(x)}$. Appling this solution to the governing equation, and neglecting higher order terms it is possible to find solutions of the form (Pierce, 1970)

$$W(x) = (\rho A)^{-\frac{3}{8}}(EI_{yy})^{-\frac{1}{8}}\left[C_1 e^{-i\int_{x_0}^{x} k_B(x)dx} + C_2 e^{-\int_{x_0}^{x} k_B(x)dx} + C_3 e^{i\int_{x_0}^{x} k_B(x)dx} + C_4 e^{\int_{x_0}^{x} k_B(x)dx}\right] \quad (2)$$

where C_1, C_2, C_3 and C_4 are arbitrary constants and the four terms correspond to positive going and negative going propagating and evanescent waves. Moreover, the exponential terms $\theta(x) = \pm\, i\int_{x_0}^{x} k_B(x)dx$ correspond to a phase change of the respective waves and $\widetilde{W}(x) = (\rho A)^{-\frac{3}{8}}(EI_{yy})^{-\frac{1}{8}}$ and $\theta(x) = \pm\int_{x_0}^{x} k_B(x)dx$ corresponds to an amplitude change because of changes in the properties of the beam and decay of evanescent waves. In terms of bending waves, $k_B(x) = (\rho A/EI_{yy})^{1/4}\sqrt{\omega}$ is the local free bending wavenumber. The phase and amplitude change of the positive going and negative going propagating and evanescent waves travelling, from $x = 0$ to $x = L$, are again related to the positive and negative going waves at the two ends i.e. $b^+ = \frac{\widetilde{W}(L)}{\widetilde{W}(0)} e^{-i\int_0^L k_B(x)dx} a^+$, $b^- = \frac{\widetilde{W}(L)}{\widetilde{W}(0)} e^{i\int_0^L k_B(x)dx} a^-$, $b_N^+ = \frac{\widetilde{W}(L)}{\widetilde{W}(0)} e^{-\int_0^L k_B(x)dx} a_N^+$, $b_N^- = \frac{\widetilde{W}(L)}{\widetilde{W}(0)} e^{\int_0^L k_B(x)dx} a_N^-$, where $\widetilde{W}(0)$ and $\widetilde{W}(L)$ are given by $\widetilde{W}(x) = (\rho A)^{-\frac{3}{8}}(EI_{yy})^{-\frac{1}{8}}$ evaluated at the points $x = 0$ and $x = L$, respectively. Then the propagation matrices are given by

$$\mathbf{\Lambda_{11}} = \begin{bmatrix} e^{-i\theta_B(0,L)+\gamma_B(0,L)} & 0 \\ 0 & e^{-\theta_B(0,L)+\gamma_B(0,L)} \end{bmatrix}, \mathbf{\Lambda_{22}} = \begin{bmatrix} e^{i\theta_B(0,L)+\gamma_B(0,L)} & 0 \\ 0 & e^{\theta_B(0,L)+\gamma_B(0,L)} \end{bmatrix}, \quad (3)$$

where $\mathbf{\Lambda_{11}}$ and $\mathbf{\Lambda_{22}}$ are the elements of the 4×4 propagation matrix $\mathbf{\Lambda}$, and

$$\theta_B(x_1, x_2) = \int_{x_1}^{x_2} k_B(x)dx \text{ and } \gamma_B(x_1, x_2) = \frac{1}{2}\ln\left[\frac{\widetilde{W}(x_2)}{\widetilde{W}(x_1)}\right], \quad (4)$$

are the phase and amplitude change, in which x_1 and x_2 are two points within the waveguide, for which $\theta_B(0, L)$ and $\gamma_B(0, L)$ are given for a wave propagating from one boundary to the other. The n^{th} natural frequency ω_n is then given from finding the n^{th} root θ_{Tn} of a transcendental equation (1) as

$$\omega_n = \frac{\theta_{Tn}^2}{\left(\int_0^L \sqrt[4]{\frac{\rho A(x)}{EI_{yy}(x)}}\, dx\right)^2}, \qquad n = 1,2,3 \ldots \quad (5)$$

3. EXPERIMENTAL ESTIMATION OF THE RANDOM FIELD PROPERTIES OF CHOPPED FIBRE COMPOSITE

In this section, a methodology for estimation of the random field properties of a panel made of glass-fibre reinforced epoxy composite material composed of chopped strand mat (CSM) is briefly reviewed (Fabro et al., 2015a). The material is randomly distributed over the panel and the distribution of Young's modulus is assumed to be isotropic. The spatial distribution correlation structure is not known *a priori* and firstly a measurement procedure, as proposed in (Gan et al., 2012), is applied to identify it.

This initial step is performed using light transmissibility measurements taken from a composite panel, from a digital image captured by a DSLR camera. An empirical relationship between the pixel values to the fibre density is used to estimate the area density AW. Assuming a constant thickness manufacturing process, the volume fraction V_f can be calculated as

$$V_f(AW) = \frac{AW}{\rho_f t}, \quad (6)$$

where ρ_f is the fibre density and t is the thickness. The random distribution of the chopped strand implies that there is no preferential direction of fibre arrangement. Therefore, it is reasonable to assume isotropy for the Young's modulus and it is possible to relate Eq. (6) to a local Young's modulus E by a simple rule of mixtures (Gan et al., 2010, Naughton et al., 1985), i.e.

$$E(E_L, E_T) = \frac{3}{8}E_L + \frac{5}{8}E_T,\ E_L(V_f) = E_f V_f + E_m(1 - V_f) \text{ and } E_T(V_f) = \left(\frac{V_f}{E_f} + \frac{1-V_f}{E_m}\right)^{-1}, \tag{7}$$

where E_f and E_m are the isotropic Young's moduli of the reinforcement fibre glass and surrounding matrix, respectively, and E_L and E_T are the longitudinal and the transverse stiffness of the mixture, respectively, for the case of a unidirectional fibre arrangement. Also, the local mass density is given by

$$\rho(V_f) = \rho_f V_f + \rho_m(1 - V_f), \tag{8}$$

where ρ_f and ρ_m are the mass densities of the reinforcement fibre glass and surrounding matrix, respectively. Table 1 summarizes the properties used for the given rule of mixtures, based on the information provided by the manufacturers of the fibre reinforcement and the epoxy resin.

E_M [GPa]	E_f [GPa]	ρ_M [kg/m^3]	ρ_f [kg/m^3]
3.2	72.3	1150	2540

Table 1. Material properties used in the rule of mixtures for the Young's modulus and mass density of the CSM.

Two panels with single and double layers of the composite were produced and the manufacturing process leads to variation in the panel thickness. It is physically reasonable to assume that the thickness correlation length is much larger than that of the volume fraction, i.e. it is significantly smoother than the volume fraction spatial distribution. Therefore, the thickness is modelled as a single random variable. It can be shown that this assumption increases the variability of the predicted natural frequencies (Fabro et al., 2015b). Measurements of the thickness are taken in a number of points over each panel, being that, in the single layer panel, the mean value is 0.468 mm and the standard deviation is 0.021 mm, and in the double layer panel, the mean value is 0.773 and the standard deviation of the thickness is 0.059 mm. More details can be found in (Fabro et al., 2015a).

The area density AW, is assumed to be a Gaussian second order homogeneous random field with mean value AW_0 and autocorrelation function $R(\tau_x, \tau_y)$, where τ_x and τ_y are the lag or delay in the x and y directions (Vanmarcke, 2010). The mean value was estimated via a sample mean over the image, and the autocorrelation function was estimated via the inverse Discrete Fourier Transform (DFT) of the two dimensional auto spectral density of the image, estimated via the segment averaging approach, using a Hann window (Newland, 2005, Shin and Hammond, 2008).

Figure 1 shows the estimated normalised autocorrelation function for the single and double layer panels respectively. Figure 2 shows the normalised autocorrelation function on the x-axis $R(\tau, 0)/R(0,0)$ and on the y-axis $R(0, \tau)/R(0,0)$ for the single and double layer panels respectively. Note that the correlation length for the single layer panel is roughly the same in all directions, i.e. it represents an isotropic correlation structure, which is expected since there might not be any preferential direction in the fibre distribution. This is not so evident for the double layer panel, and it is possible to notice a small difference in the correlation depending on the direction.

A collocation method (Ghanem and Spanos, 2012, Sudret and Der Kiureghian, 2000) was used for discretisation of the estimated two dimensional autocorrelation function $R(\tau_x, \tau_y)$ into a correlation matrix $\mathbf{R}$. This matrix was used in the associated Karhunen-Loeve (KL) eigenproblem to determine the eigenvectors $\mathbf{f}_i$ and their respective eigenvalues λ_i, such that the zero mean random field is given by

$$\mathbf{H} = \sum_{i=1}^{N_{KL}} \xi_i \sqrt{\lambda_i}\, \mathbf{f}_i, \tag{9}$$

where ξ_i is the standardized Gaussian random variable and N_{KL} is the number of terms needed in the KL expansion for an appropriate representation of the random field (Huang et al., 2001). The area density random field is then given by the matrix $\mathbf{AW} = \mathbf{AW_0} + \mathbf{H}$, whose elements refer to the pixels in the image and where $\mathbf{AW_0}$ is a matrix whose elements are equal to the random field mean value, and $\mathbf{H}$ is given by Eq. (9).

This information is used to estimate, from a single sample, the mean value and the covariance function of the spatial distribution. Furthermore, it is assumed that the fibre density random field has a Gaussian distribution and a KL expansion is used to represent it in terms of a reduced set of independent Gaussian random variables (Ghanem and Spanos, 2012, Huang et al., 2001). Figure 3 shows the Young's modulus obtained also from the rule of mixtures applied from the optical measurements for the single and double layers and Figure 4 shows the numerical simulation of the Young's modulus, also from the rule of mixtures, for the single and double layers. It can be seen qualitatively that the assumption of an area density Gaussian random field is suitable for representing the actual measurements. Details on the area density AW and mass density distribution and random field estimation can be found at (Fabro et al., 2015a)

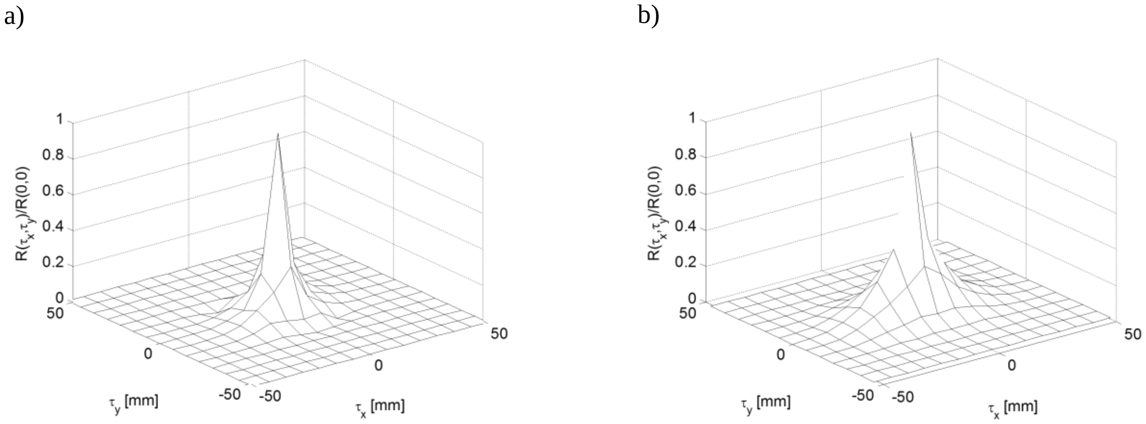

Figure 1. Normalized autocorrelation function $R(\tau_x, \tau_y)/R(0,0)$ from the area density AW spatial distribution of the (a) single and (b) double layer panel.

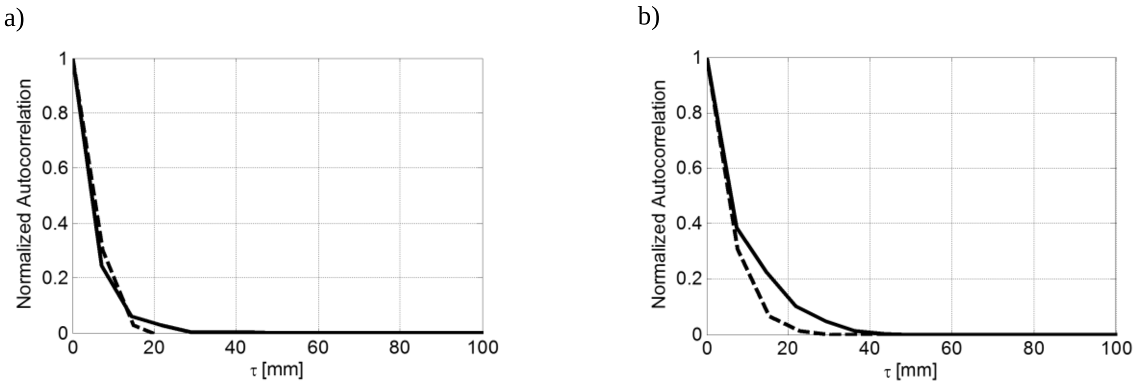

Figure 2. Normalised autocorrelation function in the x-axis $R(\tau, 0)/R(0,0)$ (dashed line) and in the y-axis $R(0, \tau)/R(0,0)$ (full line), for the (a) single and (b) double layer panel estimated from the area density spatial distribution.

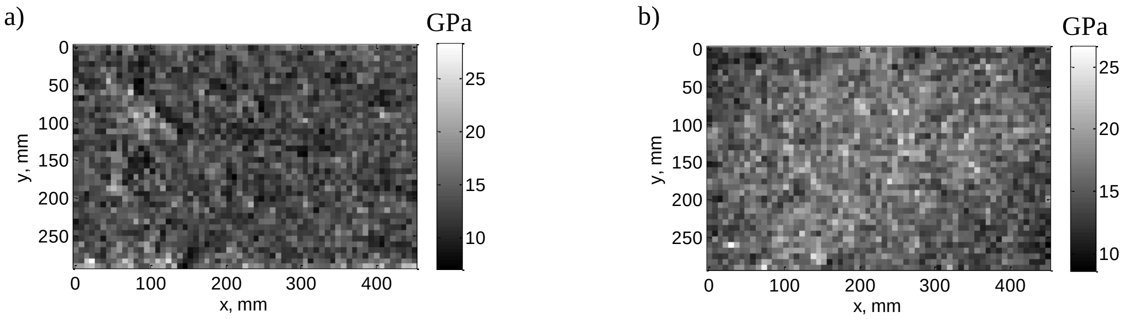

Figure 3. The Young's modulus in GPa from the optical measurements and the applied rule of mixtures at the (a) single and (b) double layer panel.

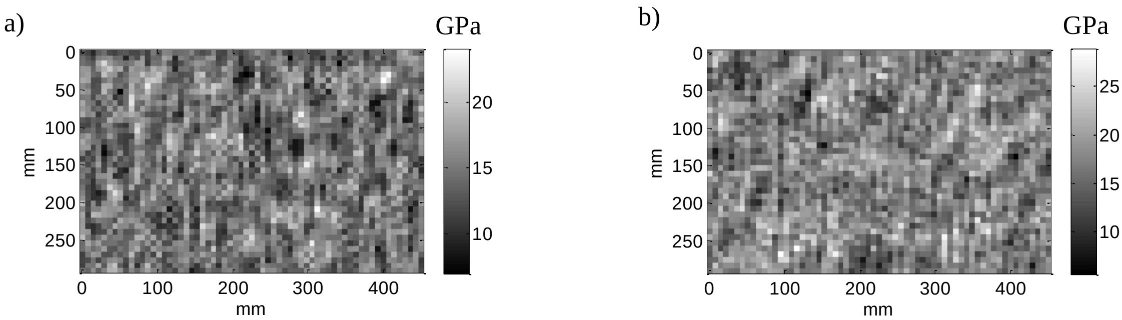

Figure 4. A numerically generated sample of the Young's modulus, in GPa, from the KL expansion and the estimated correlation function from the (a) single and (b) double layer panel.

4. EXPERIMENTAL ESTIMATION OF THE NATURAL FREQUENCIES OF THE FIBRE REINFORCED BEAMS

An experiment was set up to provide a number of frequency response functions from point measurements on the set of CSM glass fibre beams, cut from both the single and double layers panels. This set of measurements provides an ensemble to be used to assess the material variability and more details can be found in (Fabro et al., 2015a). The panels were manufactured using short chopped glass fibre reinforcement in a resin matrix and 21 samples (21×280 mm) were cut from each panel. The experiment consisted in measuring the point mobility with a Laser Doppler Vibrometer, LDV, on each beam for a hammer excitation. The vibrometer used was a Polytec PDV 100, with a sensitivity of 40mV/(mm/s), the miniature hammer, a PCB 086E80 with sensitivity 21.4 mV/N and a Dataphysics Quattro was used for the data acquisition. The beams were hung in a metallic frame using nylon string, in order to produce the free-free boundary condition and excited on the upper part with the micro hammer. A reflective tape was stuck to each beam at the position of the measurement. The measurements of the single layer beams were made from 0 to 250 Hz, with a frequency resolution of 0.3125 Hz; the double layer samples were measured from 0 to 800 Hz with a frequency resolution of 1 Hz.

The frequency response functions from the measurements on the free-free beams were calculated using the H1 estimator (Shin and Hammond, 2008), with 5 measurements for averaging the spectral density functions. The natural frequencies of the flexural modes, for each individual specimen, were identified from the mobility measurements from all of the CSM beams, using the circle-fit method (Ewins, 2000).

5. RESULTS AND DISCUSSION

The estimated random field proprieties were used to generate material proprieties samples to be used with the WKB approach applied to beams with the same dimensions than the ones cut from the CSM panels. Moreover, the same proprieties were used in a standard FE model using Euler-Bernoulli beam elements and mid-point random field discretization for benchmarking. The lowest order natural frequencies of the flexural modes obtained from the mobility measurements in the CSM beams with single and double layer are compared with the ones obtained by using the WKB approach and the identified random field.

Figure 5 presents the Coefficient of Variation, defined as $COV = \sigma_{\omega_n}/\overline{\omega}_n$, where σ_{ω_n} is the standard deviation and $\overline{\omega}_n$ is the mean value of the n^{th} natural frequency, for the single and double layer beams. Overall, the proposed models agree very well with the experimental results. The WKB approach gives the same COV for all of the modes considered, as one could expect, from Eq. (5). Moreover, the PDFs of the normalised natural frequencies are also compared with the histogram from the experimental results, for the single and double layers beams, as shown in Figures 6 and 7 for the single and double layer, respectively. The PDF for the WKB approach and the FE model also present a good agreement, although there are not enough experimental samples to compare it to the histograms.

a) b)

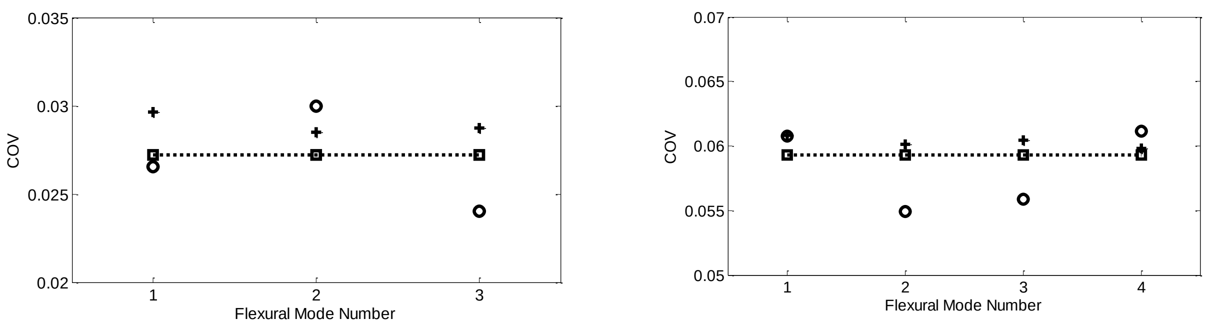

Figure 5. Coefficient of Variation COV for the lowest order flexural modes from the experimental results (circle), the FE model (+) and WKB approximation for flexural waves (square) on the CSM beams with (a) single layer and (b) double layer.

6. FINAL REMARKS

This work presented an experimental validation of the WKB approach for flexural waves in predicting the natural frequencies of beam with random spatially varying properties. The beams were made of a glass-fibre reinforced epoxy composite material composed of chopped strand mat (CSM) with the area density modelled as a random field with properties estimated from a light transmissibility measurement procedure. A rule of mixture was then applied to calculate the material properties which were, in turn, used in the WKB approach. Experimental measurements of the statistics of the natural frequencies of the beams presented a very good agreement with the results obtained from the WKB approach and standard FE models used for benchmarking.

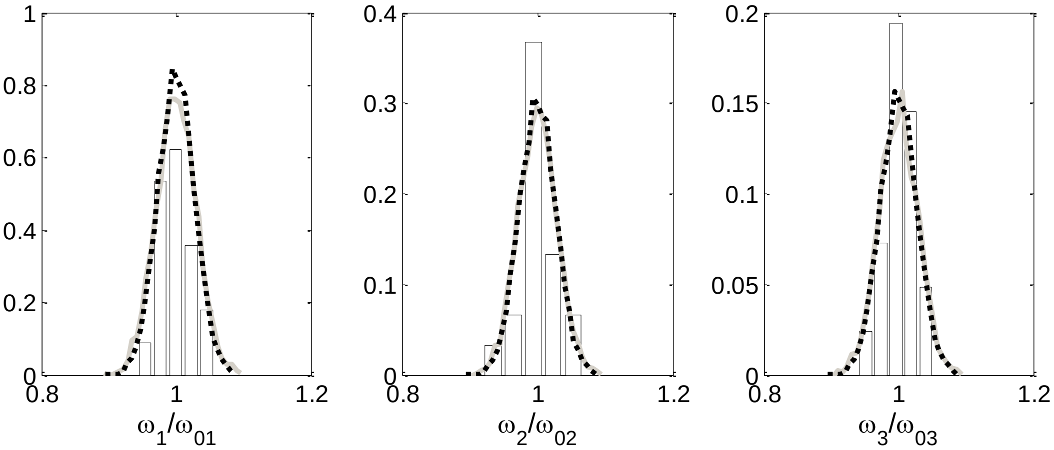

Figure 6. Normalized natural frequency PDFs for the lowest three flexural modes from the experimental results (bars), the FE model (grey) and WKB approximation (dashed) on the single layer CSM beams.

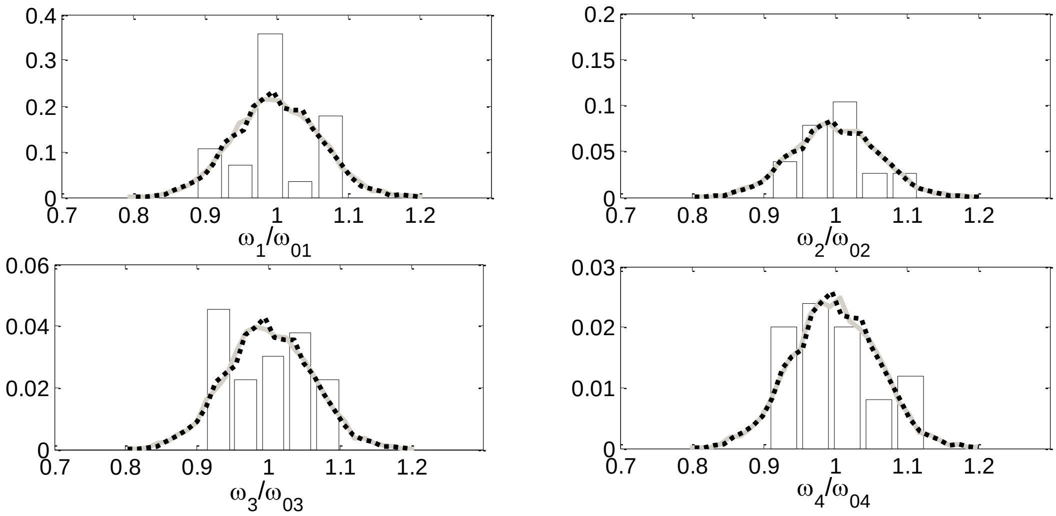

Figure 7. Normalized natural frequency PDFs for the lowest three flexural modes from the experimental results (bars), the FE model (grey) and WKB approximation (dashed) on the double layer CSM beams.

7. ACKNOWLEDGEMENTS

The authors gratefully acknowledge the financial support of the Brazilian National Council of Research (CNPq), Process number 445773/2014-6 and 237801/2012-4.

8. REFERENCES

Arenas J.P., Crocker M.J., 2001, "A note on a WKB application to a duct of varying cross-section", *Appl. Math. Lett.* Vol. 14, pp. 667–71

Cremer L., Heckl M., Petersson B.A.T., 2010, "Structure-borne sound: Structural vibrations and sound radiation at audio frequencies", Berlin, Germany: Springer

Deraemaeker A., Babuška I., Bouillard P., 1999, "Dispersion and pollution of the FEM solution for the Helmholtz equation in one, two and three dimensions", *Int. J. Numer. Methods Eng.* Vol. 46, pp. 471–99

Der Kiureghian A., Ke J.-B., 1988, "The stochastic finite element method in structural reliability", *Probabilistic Eng. Mech.* Vol. 3, pp. 83–91

Eisenberger M., 1991, "Exact longitudinal vibration frequencies of a variable cross-section rod", *Appl. Acoust.* Vol. 34, pp. 123–30

Ewins D.J., 2000, "Modal Testing: Theory, Practice and Application", Bognor Regis, England: John Wiley & Sons Ltda. 561 pp.

Fabro A.T., Ferguson N.S., Gan J.M., Mace B.R., Bickerton S., Battley M., 2015a, "Estimation of random field material properties for chopped fibre composites and application to vibration modelling", *Compos. Struct.* Vol. 125, pp. 1–12

Fabro A.T., Ferguson N.S., Jain T., Halkyard R., Mace B.R., 2015b, "Wave propagation in one-dimensional waveguides with slowly varying random spatially correlated variability", *J. Sound Vib.* Vol. 343, pp. 20–48

Firouz-Abadi R.D., Haddadpour H., Novinzadeh A.B., 2007, "An asymptotic solution to transverse free vibrations of variable-section beams", *J. Sound Vib.* Vol. 304, pp. 530–40

Gangadhar M., Zehn M.W., 2007, "A methodology to model spatially distributed uncertainties in thin-walled structures", *ZAMM - J. Appl. Math. Mech. Z. Für Angew. Math. Mech.* Vol. 87, pp. 360–76

Gan J.M., Bickerton S., Battley M., 2010, "Automated characterization of variability in glass fibre reinforcement architecture" In: Proceeding of the 10th International Conference on Textile Composites – TEXCOMP10, Lille, France, p. 148–56

Gan J.M., Bickerton S., Battley M., 2012, "Quantifying variability within glass fibre reinforcements using an automated optical method", *Compos. Part Appl. Sci. Manuf.* Vol. 43, No. 8, pp. 1169–76

Gaulter S.N., Biggs N.R.T., 2012, "Acoustic trapped modes in a three-dimensional waveguide of slowly varying cross section", *Proc. R. Soc. Math. Phys. Eng. Sci.*, doi:10.1098/rspa.2012.0384

Ghanem R., Spanos P.D., 2012, "Stochastic Finite Elements: A Spectral Approach", Minneola, N.Y.: Dover Publications. 240 pp. Revised edition ed.

Guo S., Yang S., 2012, "Wave motions in non-uniform one-dimensional waveguides", *J. Vib. Control*. Vol. 18, pp. 92–100

Huang S.P., Quek S.T., Phoon K.K., 2001, "Convergence study of the truncated Karhunen–Loeve expansion for simulation of stochastic processes", *Int. J. Numer. Methods Eng.* Vol. 52, pp. 1029–43

Jensen F.B., Kuperman W.A., Porter M.B., Schimidt H., 2011, "Computational Ocean Acoustics", New York: Springer

Lei H.F., Zhang Z.Q., Liu B., 2012, "Effect of fiber arrangement on mechanical properties of short fiber reinforced composites", *Compos. Sci. Technol.* Vol. 72, pp. 506–14

Li Q.S., 2000, "Exact solutions for free longitudinal vibrations of non-uniform rods", *J. Sound Vib.* Vol. 234, pp. 1–19

Mace B.R., 1984, "Wave reflection and transmission in beams", *J. Sound Vib.* Vol. 97, pp. 237–46

Naughton B.P., Panhuizen F., Vermeulen A.C., 1985, "The elastic properties of chopped strand mat and woven roving in g.r. laminae", *J. Reinf. Plast. Compos.* Vol. 4, pp. 195–204

Nayfeh A.H., 1973, "Perturbation methods", New York: Wiley

Newland D.E., 2005, "An introduction to random vibrations, spectral & wavelet analysis", Mineola, NY: Dover Publications

Pierce A.D., 1970, "Physical interpretation of the wkb or eikonal approximation for waves and vibrations in inhomogeneous beams and plates", *J. Acoust. Soc. Am.* Vol. 48, pp. 275–84

Rienstra S.W., 2003, "Sound propagation in slowly varying lined flow ducts of arbitrary cross-section", *J. Fluid Mech.* Vol. 495, pp. 157–73

Schueller G.I., 1997, "A state-of-the-art report on computational stochastic mechanics", *Probabilistic Eng. Mech.* Vol. 12, pp. 197–321

Shin K., Hammond J.K., 2008, "Fundamentals of Signal Processing for Sound and Vibration Engineers", Chichester, England: John Wiley & Sons Inc.

Smarslok B.P., Haftka R.T., Ifju P.G., 2012, "Correlation model for composite elastic properties using only measurements from a single specimen", *Probabilistic Eng. Mech.* Vol. 29, pp. 64–69

Sriramula S., Chryssanthopoulos M.K., 2009, "Quantification of uncertainty modelling in stochastic analysis of frp composites", *Compos. Part Appl. Sci. Manuf.* Vol. 40, pp. 1673–84

Stefanou G., 2009, "The stochastic finite element method: past, present and future", *Comput. Methods Appl. Mech. Eng.* Vol. 198, pp. 1031–51

Sudret B., Der Kiureghian A., 2000, "Stochastic finite element methods and reliability: a state-of-art report", *UCB/SEMM-2000/08*, University of California, Berkeley

Vanmarcke E., 2010, "Random Field: Analysis and Synthesis", Cambridge, MA: Word Scientific. 2nd Revised and Expanded ed.

Zehn M.W., Saitov A., 2003, "How can spatially distributed uncertainties be included in fea and in parameter estimation for model updating?", *Shock Vib.* Vol. 10, pp. 15–25

9. RESPONSIBILITY NOTICE

The authors are only responsible for the printed material included in this paper.